# Climate response to volcanic forcing: Validation of climate sensitivity of a coupled atmosphere-ocean general circulation model

T. Yokohata,[1] S. Emori,[1,2] T. Nozawa,[1] Y. Tsushima,[2] T. Ogura,[1] and M. Kimoto[3]

Received 18 May 2005; revised 29 July 2005; accepted 23 September 2005; published 5 November 2005.

[1] Two versions of a coupled atmosphere-ocean general circulation model (GCM) with different climate sensitivities are tested on global cooling following the Pinatubo volcanic eruption to investigate the validity of high climate sensitivities. The higher-sensitivity version, with climate sensitivity of 6.3 K for doubled $CO_2$ forcing, overestimates cooling due to the volcanic eruption, whereas the lower-sensitivity version (4.0 K) produces results consistent with observations. A simple scheme for climate feedback analysis is devised and it is found that the difference between the two versions is attributed to cloud-albedo feedback. This validation method is expected to provide additional constraints on climate sensitivity and possibly lead to reduced uncertainties in climate prediction.
**Citation:** Yokohata, T., S. Emori, T. Nozawa, Y. Tsushima, T. Ogura, and M. Kimoto (2005), Climate response to volcanic forcing: Validation of climate sensitivity of a coupled atmosphere-ocean general circulation model, *Geophys. Res. Lett.*, *32*, L21710, doi:10.1029/2005GL023542.

## 1. Introduction

[2] Climate sensitivity, defined in the present study as the equilibrium response of global mean surface air temperature to doubling of the atmospheric $CO_2$ concentration, is one of the most important features of numerical models for future climate projection [*Intergovernmental Panel on Climate Change*, 2001]. Reducing the uncertainty in the climate sensitivity by simply testing a model's ability to simulate the mean present-day climate is difficult; recently, *Stainforth et al.* [2005] have shown that the climate sensitivity may be anywhere from 2 K to 11 K and the high end cannot be rejected.

[3] Climate sensitivity can also be tested by comparison of modeled and observed historical climate changes on the time scale of multiple years, such as global cooling after large volcanic eruptions [e.g., *Wigley et al.*, 2005], or on much longer time scales, such as the global warming trend in the late twentieth century [e.g., *Forest et al.*, 2002]. However, the studies so far of both types have employed simple energy balance models, and thus have been unable to consider cloud processes explicitly, which are expected to play a key role in determining climate sensitivity [*Cess et al.*, 1990]. Studies of the latter type includes appreciable uncertainty mainly related to historical forcing, and thus the results tend to accept the possibility of high sensitivities (6 K or higher). Simulations of volcanic cooling using a GCM have not been considered to date as a test of climate sensitivity, although tests of water vapor feedback have been done [e.g., *Soden et al.*, 2002].

[4] In this study, the simulations of climate response to the volcanic eruptions of Mount Pinatubo in 1991 are performed using two versions of a coupled atmosphere-ocean GCM [*K-1 Model Developers*, 2004] with climate sensitivities of 4.0 K (lower-sensitivity, LS) and 6.3 K (higher-sensitivity, HS), and compared with the observations. While the two versions differ only in the treatment of clouds, both of them provide realistic simulations of the mean present-day climate [*Ogura et al.*, 2005].

## 2. Model and Experiments

[5] The coupled atmosphere-ocean GCM employed is MIROC version 3.2 [*K-1 Model Developers*, 2004]. The spatial resolution of the atmospheric component is T42 with 20 levels (the height of the model top is approximately 30 km), while that of the ocean component is 1.4° longitude by variable 0.56–1.4° latitude with 44 levels. The Pinatubo experiment (PNTB) consists of control and perturbed sets of ensemble runs. The control runs were integrated under the preindustrial (1850) condition for more than 600 years. The perturbed runs were performed for a period of 10 years with volcanic forcing based on the stratospheric aerosol optical thickness at 550 nm [*Hansen et al.*, 2002] imposed on the control condition. Four-member-ensemble runs were performed using different initial conditions picked from the control run.

[6] We also use the doubled $CO_2$ experiment (2XCO2) performed to measure the climate sensitivity [*Ogura et al.*, 2005] for the feedback analysis. The control runs (285 ppm $CO_2$) and the perturbed runs with the doubled atmospheric $CO_2$ concentration (570 ppm) were performed by using the atmospheric part of the coupled GCM with a mixed-layer ocean model until the system reaches equilibrated states [*Ogura et al.*, 2005].

## 3. Response to Pinatubo Eruption

[7] The time series of globally averaged surface air temperature (SAT) in the PNTB is shown in Figure 1. Both versions indicate cooling after the volcanic eruption. Compared to the HS version, the LS version exhibits less cooling and a shorter recovery time. This result is consistent with that of the 2XCO2, in which the LS version has smaller SAT response. The difference between the LS and HS

[1]Atmospheric Environment Division, National Institute for Environmental Studies, Tsukuba, Japan.
[2]Frontier Research Center for Global Change, Japan Agency for Marine-Earth Science and Technology, Yokohama, Japan.
[3]Center for Climate System Research, University of Tokyo, Kashiwa, Japan.

Copyright 2005 by the American Geophysical Union.
0094-8276/05/2005GL023542$05.00

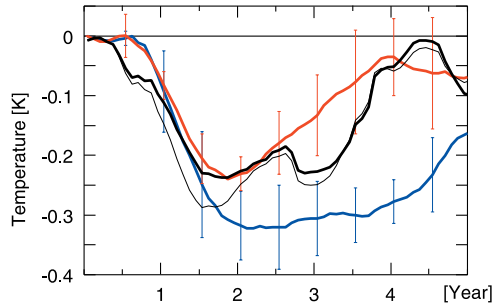


**Figure 1.** Anomaly time series of global mean surface air temperature (SAT) after the Pinatubo volcanic eruption simulated by model versions with climate sensitivity of 4.0 K (LS, red) and 6.3 K (HS, blue). SAT observations by HadCRUT2v [*Jones and Moberg*, 2003] with the linear trend from 1981 to 2000 removed (thick black) and that with the ENSO signal additionally removed (thin black) are also shown. Modeled and observed anomalies are calculated by taking the mean of 12 months prior to the eruption as a baseline. The global mean was computed by taking the area-weighted average in the region where observational data are available. The time series are smoothed by a 12-month moving average, and error bars denote the standard deviation of the model ensembles.

versions becomes larger than the ensemble standard deviations approximately two years after the eruption.

[8] The ensemble means of the two versions are compared to the observed SAT change [*Jones and Moberg*, 2003] in Figure 1. From the observed SAT time series, the linear trend from 1981 to 2000 is removed to exclude the effects of greenhouse gases (GHGs) and aerosols. The observed time series with the El Niño Southern Oscillation (ENSO) signal additionally removed by the method of *Santer et al.* [2001] is also shown in Figure 1. The ENSO signal was not removed from the simulated time series because it should be canceled, to some extent, in the ensemble mean and because it cannot be removed properly by that method; since the simulated ENSO index contains the volcanic signal due to the underestimated amplitude of the modeled ENSO, the volcanic signal (as well as the ENSO signal) would also be removed from the SAT time series.

[9] Compared to the HS version, the LS version shows better agreement with the observations (Figure 1). The time series of the observation (both with and without the ENSO signal) settle almost within the range of the ensemble standard deviation of the LS version, but not for the HS version. This result suggests that the HS version fails to explain the observations.

[10] The SAT response discussed above depends not only on the climate sensitivity of the model, but also on the radiative forcing imposed on the model. It has also been confirmed that the radiative forcings by the LS and HS versions are almost identical (less than 0.1 $Wm^{-2}$ difference) and are consistent with the estimation by *Hansen et al.* [2002]. Although other estimates of the radiative forcing for the Pinatubo event have been reported [e.g., *Andronova et al.*, 1999], these alternative estimates are generally lager than the forcing imposed in the present work. Therefore, the LS version would not be as consistent with the observations as shown in the present result if higher estimates of forcing were employed. However, the better agreement of the LS version than the HS version with the observations and the inability of the HS version to explain the observations would not change for the higher forcing estimates.

## 4. Feedback Analysis

[11] A simple scheme was devised to diagnose feedback processes. For the shortwave (SW) radiative feedbacks, our scheme mitigates a problem in the conventional scheme using the cloud radiative forcing (CRF) method [e.g., *Colman*, 2003]. This is important especially for the PNTB, in which the SW CRF can change even though clouds do not change from the control to perturbed runs, because the SW flux incident upon clouds changes owing to the volcanic aerosols. Among the many feedback diagnoses developed to date [e.g., *Colman*, 2003], our scheme is useful in that major feedbacks are evaluated from a straightforward calculation using the conventional model output. Detailed explanation and validation of the scheme can be found in work by *Yokohata et al.* [2005], where an updated version of the present scheme is described.

[12] The strength of the feedback processes is evaluated from the SW and longwave (LW) radiative anomalies (calculated by the difference between the perturbed and control runs) at the top of the atmosphere (TOA) broken down into contributions from the surface, clear-sky atmosphere defined as the part of the atmosphere except clouds, and clouds ($\Delta F_i^j$, where $i$ = sfc, clr, cld and $j$ = sw,lw, see Appendix A for details). Responses due to feedback processes ($\Delta R_i^j$) are computed by $\Delta F_i^j - \Delta G_i^j$, where $\Delta G_i^j$ is the radiative forcing component, calculated from the instantaneous radiative forcing at the TOA [*Hansen et al.*, 2002] broken down into the components in the same way as the $\Delta F_i^j$. Then, we can represent the globally averaged energy budget at the TOA as $\partial H/\partial t = \sum_{i,j}[\overline{\Delta G_i^j} + \gamma_i \overline{\Delta T}]$, where $H$ represents the heat content of the atmosphere-ocean system,

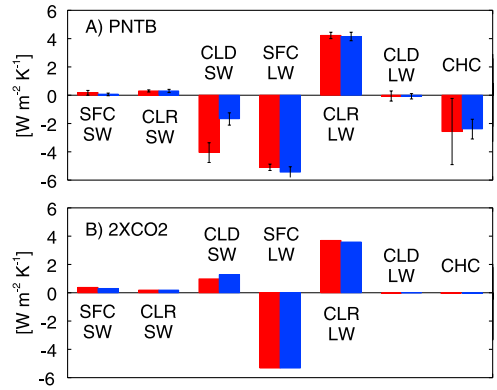


**Figure 2.** The response parameters for the (a) Pinatubo experiment and (b) doubled $CO_2$ experiment, showing results for the LS (red) and HS (blue) versions. Bars represent the response parameter for the SW and LW anomalies due to the surface (SFC), clear-sky atmosphere (CLR), and clouds (CLD). The change in the heat content (CHC) is also shown. Error bars denote the standard deviations of the model ensembles.

the overline denotes the global average, $\Delta T$ is the anomaly in the SAT, and $\gamma_i^j$ is the response parameter calculated by $\overline{\Delta R_i^j}/\overline{\Delta T}$ (the negative value of which represents a damping or negative feedback, while the positive represents a positive feedback). We can evaluate the ice-albedo feedback by $\gamma_{\mathrm{sfc}}^{\mathrm{sw}}$, cloud feedbacks by $\gamma_{\mathrm{cld}}^{\mathrm{sw}}$ and $\gamma_{\mathrm{cld}}^{\mathrm{lw}}$, Stefan-Boltzmann damping by $\gamma_{\mathrm{sfc}}^{\mathrm{lw}}$, and combined water vapor and lapse rate feedback by $\gamma_{\mathrm{clr}}^{\mathrm{lw}}$.

[13] In Figure 2, the response parameters in the PNTB and 2XCO2 are shown. The former is the time-averaged values during the $\gamma_i^j$ are almost temporally constant (1–2.5 yr after the eruption with 1 yr prior to it taken as a baseline) to represent the transient response of the PNTB. The latter is the difference between the equilibrated states of the perturbed and control runs. The values of $\partial H/\partial t$ over $\Delta T$, which correspond to the change in the heat content are also shown in Figure 2.

[14] Both experiments show that the strongest factors are the response parameter for the Stefan-Boltzmann damping (SFC-LW), the water vapor and lapse late feedback (CLR-LW), and the cloud albedo feedback (CLD-SW). In the PNTB, the change in the heat content (CHC) also has a large value. The other factors are relatively minor.

[15] The SFC-LW and CLR-LW are similar in the PNTB and 2XCO2. The CLD-SW is negative in the PNTB, yet positive in the 2XCO2. This difference in sign can be mainly attributed to the latitudinal distribution of forcing, and possibly to the transient nature of the PNTB. The negative feedback over the tropics works effectively in the PNTB because the volcanic forcing centered on the tropics reduces convection and the formation of anvil clouds. In the 2XCO2, on the other hand, the signal of cloud reduction over the subtropics overwhelms that of cloud increase in the tropics, leading to a positive feedback. In addition, the CHC is negative in the PNTB, which might be related to the negative value of the CLD-SW. It needs further investigation as an important future work.

[16] In both the PNTB and 2XCO2, the maximum difference in the response parameter between the two versions occurs in CLD-SW. This difference can be attributed to the cloud response at the mid-to-high latitudes, where the LS version produces more negative feedback than the HS version in both experiments (the details can be found in the auxiliary material[1]). This result is consistent with that by *Ogura et al.* [2005], who conducted a detailed analysis of the cloud response to doubled $CO_2$ forcing using the two versions of this model.

[17] The cloud albedo feedback in the LS and HS versions can be validated in Table 1 by calculating the SW anomaly due to clouds ($\Delta F_{\mathrm{cld}}^{\mathrm{sw}}$, positive defined as downward direction) following the Pinatubo eruption using the radiative flux estimated from the globally observed data set, ISCCP-FD [*Zhang et al.*, 2004]. The time-averaged values are taken using the same period as that in the Figure 2. From the values of ISCCP-FD, the linear trend from 1981 to 2000 is removed to exclude the effects of GHGs and aerosols. The $\Delta F_{\mathrm{cld}}^{\mathrm{sw}}$ by LS version appears to be closer to reality, considering the suspected overestimation of the SW reflection by clouds following the Pinatubo eruption (i.e., underestimation of $\Delta F_{\mathrm{cld}}^{\mathrm{sw}}$) in the ISCCP-FD data [*Zhang et al.*, 2004].

**Table 1.** Anomaly in SW Flux ($\mathrm{Wm}^{-2}$) Due to Clouds Following the Pinatubo Eruption for ISCCP-FD, LS and HS[a]

| | ISCCP-FD | LS | HS |
|---|---|---|---|
| $\Delta F_{\mathrm{cld}}^{sw}$ | 0.64 | 0.90 ± 0.25 | 0.47 ± 0.08 |

[a]Here ± refers to the simulated ensemble standard deviation.

## 5. Summary and Conclusions

[18] On the basis of this feedback analysis, the difference in the global mean SAT response between the LS and HS versions appears to originate mainly from the cloud-albedo feedback, in both the PNTB and 2XCO2. Although the sign in the cloud-albedo feedback differs between the two experiments (negative in PNTB and positive in 2XCO2), the LS version consistently produces a more negative feedback than the HS version in the two experiments (smaller negative in PNTB and larger positive in 2XCO2). As the factor that determines the difference between the LS and HS versions in the PNTB and 2XCO2 is the same (i.e., cloud-albedo feedback), the reliability of the LS and HS versions in the 2XCO2 can be reasonably tested by the results of the PNTB.

[19] The global mean SAT response of the LS version to the Pinatubo forcing is in better agreement with the observations than the HS version. The cloud-albedo feedback of the LS version after the Pinatubo eruption is also likely to be more consistent with the observations. Therefore, the climate response of the LS version is considered to be more reliable, and thus the climate sensitivity of the LS version (4.0 K) is expected to be more reasonable than that of the HS version (6.3 K).

[20] The climate sensitivity could differ among climate models for various reasons, not necessarily due solely to differences in the cloud-albedo feedback. Therefore, the present results should only be valid for models in which the climate sensitivity is strongly dependent on the cloud-albedo feedback. However, the present work demonstrates that it is possible to test the likelihood of climate sensitivity by hindcasting the historical climate changes. This validation method for climate models is therefore expected to improve our understanding of the uncertainty in climate sensitivity.

## Appendix A: Simple Feedback Analysis Scheme

[21] The method to break down the SW and LW anomaly at the TOA into contributions from the surface, the clear-sky atmosphere, and clouds is described below. For the SW formulation, the net SW flux at the TOA of the model output ($F_{\mathrm{t}}^{\mathrm{sw}}$, positive defined as downward direction) is divided into contributions from the surface and the full-sky atmosphere, as shown in Figure A1 and expressed as

$$F_{\mathrm{t}}^{\mathrm{sw}} = F_{\mathrm{t}\downarrow}^{\mathrm{sw}} - A_{\mathrm{sfc}} T_{\mathrm{ful}}^2 F_{\mathrm{t}\downarrow}^{\mathrm{sw}} - A_{\mathrm{ful}} F_{\mathrm{t}\downarrow}^{\mathrm{sw}} \quad \text{(A1)}$$

where $A$ and $T$ denote the albedo and transmissivity of the surface (sfc) and full-sky atmosphere (ful), and $F_{\mathrm{t}\downarrow}^{\mathrm{sw}}$ is the downward SW flux at the TOA. In formulating equation

[1]Auxiliary material is available at ftp://ftp.agu.org/apend/gl/2005GL023542.

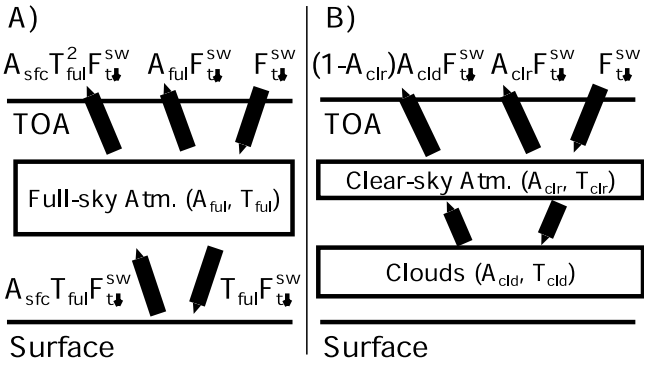


**Figure A1.** (a) Formulation for breaking down the SW flux at the TOA into contributions from the surface and full-sky atmosphere. (b) Relationship between the SW albedo of the full-sky and clear-sky atmosphere, and clouds based on a simple two-layer model. Explanations of the variables can be found in the main text.

(A1), it is assumed that the ratio of the atmospheric transmissivity to downward and upward SW fluxes to be unity for simplicity. As the variables in equation (A1) other than $A_{\mathrm{ful}}$ can be obtained from the conventional model output ($A_{\mathrm{sfc}}$ by the ratio between the upward and downward SW fluxes at the surface, $T_{\mathrm{ful}}$ by the ratio between the full-sky downward SW fluxes at the surface and at the TOA), it is possible to find $A_{\mathrm{ful}}$. The clear-sky values $A_{\mathrm{clr}}$ and $T_{\mathrm{clr}}$ can also be found by formulating the clear-sky net SW flux at the TOA in the same way as equation (A1).

[22] The albedo and transmissivity of the full-sky atmosphere can then be presented as functions of clear-sky atmosphere and cloudy ($A_{\mathrm{cld}}$ and $T_{\mathrm{cld}}$) values. For this purpose, a simple two-layer model is assumed as shown in Figure A1 and described by

$$A_{\mathrm{ful}} = A_{\mathrm{clr}} + (1 - A_{\mathrm{clr}})A_{\mathrm{cld}} \quad \text{and} \quad T_{\mathrm{ful}} = T_{\mathrm{clr}}T_{\mathrm{cld}}. \tag{A2}$$

$A_{\mathrm{cld}}$ and $T_{\mathrm{cld}}$ can be derived from equation (A2).

[23] By substituting equation (A2) into equation (A1) and obtaining the perturbation, the anomaly in $F_{\mathrm{t}}^{\mathrm{sw}}$ can be calculated as follows.

$$\begin{aligned}\Delta F_{\mathrm{t}}^{\mathrm{sw}} = &-\Delta A_{\mathrm{s}}(T_{\mathrm{clr}}T_{\mathrm{cld}})^2F_{\mathrm{t}\downarrow}^{\mathrm{sw}} \\ &- 2T_{\mathrm{clr}}\Delta T_{\mathrm{clr}}\left(A_{\mathrm{sfc}}T_{\mathrm{cld}}^2\right)F_{\mathrm{t}\downarrow}^{\mathrm{sw}} - (1 - A_{\mathrm{cld}})\Delta A_{\mathrm{clr}}F_{\mathrm{t}\downarrow}^{\mathrm{sw}} \\ &- 2T_{\mathrm{cld}}\Delta T_{\mathrm{cld}}\left(A_{\mathrm{sfc}}T_{\mathrm{clr}}^2\right)F_{\mathrm{t}\downarrow}^{\mathrm{sw}} - (1 - A_{\mathrm{clr}})\Delta A_{\mathrm{cld}}F_{\mathrm{t}\downarrow}^{\mathrm{sw}}\end{aligned} \tag{A3}$$

where $\Delta$ denotes the difference between the perturbed and control runs, and the other values are those of the control run. The term on the first line of equation (A3) is regarded as the contribution from the surface, those on the second line represent the clear-sky-atmosphere contribution, and those on the third line are the cloud contribution ($\Delta F_{\mathrm{cld}}^{\mathrm{sw}}$ in Table 1).

[24] For the LW formulation, the conventional scheme is adopted because LW processes include emission as well as absorption and are very complicated. The surface contribution is formulated as the conventional Stefan-Boltzmann damping by the anomaly in the upward LW flux at the surface. The clear-sky atmospheric contribution is formulated as the atmospheric greenhouse effect [e.g., *Meehl et al.*, 2004] by the anomaly in the difference between the upward LW flux at the surface and the clear-sky upward LW flux at the TOA. The contribution from clouds is formulated as the conventional cloud radiative forcing [e.g., *Cess et al.*, 1990] by the anomaly in the difference between the full-sky and clear-sky LW fluxes at the TOA.

[25] **Acknowledgments.** This work was supported by the Research Revolution 2002 (RR2002) of the Ministry of Education, Sports, Culture, Science and Technology of Japan, and by the Global Environment Research Fund (GERF) of the Ministry of the Environment of Japan. Model calculations were made on an NEC SX-6 at NIES and the Earth Simulator.

## References

Andronova, N. G., E. V. Rozanov, F. Yand, M. E. Schlesinger, and G. L. Stenchikov (1999), Radiative forcing by volcanic aerosols from 1850 to 1994, *J. Geophys. Res.*, *104*, 16,807–16,826.

Cess, R. D., et al. (1990), Intercomparison and interpretation of climate feedback processes in 19 atmospheric general circulation models, *J. Geophys. Res.*, *95*, 16,601–16,615.

Colman, R. A. (2003), A comparison of climate feedbacks in general circulation model, *Clim. Dyn.*, *20*, 865–873.

Forest, C. E., P. H. Stone, A. P. Sokolov, M. R. Allen, and M. D. Webster (2002), Quantifying uncertainties in climate system properties with the use of recent climate observations, *Science*, *295*, 113–117.

Hansen, J., et al. (2002), Climate forcing in Goddard Institute for Space Studies SI2000 simulations, *J. Geophys. Res.*, *107*(D18), 4347, doi:10.1029/2001JD001143.

K-1 Model Developers (2004), K-1 coupled GCM (MIROC) description, *K-1 Tech. Rep. 1*, edited by H. Hasumi and S. Emori, Univ. of Tokyo, Tokyo.

Intergovernmental Panel on Climate Change (2001), *Climate Change 2001: The Scientific Basis*, edited by J. T. Houghton et al., 944 pp., Cambridge Univ. Press, New York.

Jones, P. D., and A. Moberg (2003), Hemispheric and large-scale surface air temperature variations: An extensive revision and an update to 2001, *J. Clim.*, *16*, 206–223.

Meehl, G. A., W. M. Washington, J. M. Arblaster, and A. Hu (2004), Factors affecting climate sensitivity in global coupled models, *J. Clim.*, *17*, 1584–1596.

Ogura, T., S. Emori, Y. Tsushima, T. Yokohata, A. Abe-Ouchi, and M. Kimoto (2005), Climate sensitivity of a general circulation model with different cloud modelling assumptions, Climate sensitivity of a general circulation model with different cloud modelling assumptions, paper presented at IAMAS 2005 Scientific Assembly, Int. Assoc. of Meteorol. and Atmos. Sci., Beijing, 2–11 Aug.

Santer, B. D., T. M. L. Wigley, C. Doutriaux, J. S. Boyle, J. E. Hansen, P. D. Jones, G. A. Meehl, E. Roeckner, S. Sengupta, and K. E. Taylor (2001), Accounting for the effects of volcanos and ENSO in comparisons of modeled and observed temperature trends, *J. Geophys. Res.*, *106*, 28,033–28,059.

Soden, B. J., R. T. Wetherald, G. L. Stenchikov, and A. Robock (2002), Global cooling after the eruption of Mt. Pinatubo: A test of climate feedback by water vapor, *Science*, *296*, 727–730.

Stainforth, D. A., et al. (2005), Uncertainty in predictions of the climate response to rising levels of greenhouse gases, *Nature*, *433*, 403–406.

Wigley, T. M. L., C. M. Amman, B. D. Santer, and S. C. B. Raper (2005), The effect of climate sensitivity on the response to volcanic forcing, *J. Geophys. Res.*, *110*, D09107, doi:10.1029/2004JD005557.

Yokohata, T., S. Emori, T. Nozawa, Y. Tsushima, T. Ogura, and M. Kimoto (2005), A simple scheme for climate feedback analysis, *Geophys. Res. Lett.*, *32*, L19703, doi:10.1029/2005GL023673.

Zhang, Y., W. B. Rossow, A. A. Lacis, V. Oinas, and M. I. Mishchenko (2004), Calculation of radiative fluxes from the surface to top of atmosphere based on ISCCP and other global data sets: Refinements of the radiative transfer model and the input data, *J. Geophys. Res.*, *109*, D19105, doi:10.1029/2003JD004457.

S. Emori, T. Nozawa, T. Ogura, and T. Yokohata, Atmospheric Environment Division, National Institute for Environmental Studies, 16-2, Onogawa, Tsukuba, Ibaraki 305-8506, Japan. (yokohata.tokuta@nies.go.jp)

M. Kimoto, Center for Climate System Research, University of Tokyo 5-1-5, Kashiwanoha, Kashiwa, Chiba 277-8568, Japan.

Y. Tsushima, Frontier Research Center for Global Change, Japan Agency for Marine-Earth Science and Technology, 3173-25, Showa-machi, Kanazawa-ku, Yokohama, Kanagawa 236-0001, Japan.